Transient Temperature Responses in Pulsed Microwave Diodes

Yoh-ichiro OGITA

Dept. of Electrical Engineering, Ikutoku Techinical University, Atsugi 243-02

Abstract

A thermal model is proposed to estimate transient temperature responses and spatial temperature distributions in pulsed microwave oscillation diodes such as TRAPATT, IMPATT and GUNN diodes. Turn-on and turn-off temperature transients calculated from this model are compared with that calculated by published methods and also with experimental results, to show the valaidity of this analysis. The transients calculated from this model with temperature dependences of thermal constants are compared with that without these dependences ; it is shown that the analysis neglecting those dependences does not cause a large error in the temperature transient in the ranging 0 to 200℃. The diode chip area and metallic contact thickness dependences of the thermal resistance at the junction are presented. The diode-chip-length and pulse width dependences of the thermal resistance, propagation characteristics of heat and power flux through the chip, are presented and discussed. A useful relation for the thermal design of the pulsed diodes, between the setting place of the heat sink and pulse width applied is presented for Si and GaAs, to indicate the condition to get sink effect efficiently due to the heat sink. The possibility of the suppression of the temperature variation during a pulse is discussed from the standpoint of the thermal design techniques. It is shown that the variation decreases over the entire pulse width by means of the appropriate combining the propagation delay effect of the heat through the diode chip with the sink effect due to the heat sink.

1. Introduction

Microwave plused oscillators utilizing TRAPATT, IMPATT, and GUNN diodes usually have an oscillation frequency and output power variation in a pulse duration [1-3]. Such variations cause a phase and frequency error to make a locking bandwidth narrow in injection locked amplifiers utilizing such oscillators† [4-6]. Such narrow locking width causes some problems in systems using these oscillators, such as, radar beacon, FM pulsed radar and active phased array radar [3-8]. Several considerations have been made for suppresssing these variations from standpoints of circuit design† [1], [4], [7], [8] and device design [3], [9]. However, it is found hard to eliminate these variations completely from such standpoints, since the above variations are drastically affected by the transient variations of the junction temperature of diodes [3], [7], [9], [10]. Hence, in addition to the above methods,

* Received Oct. 6, 1983

† Contribution entitled "Study on injection locking amplfiers by use of TRAPATT oscillators having frequency variation during a pulse" has been presented by author on 5th Specialist Workshop on "Avtive Microwave Semiconductor Devices" in Italy, Oct., 1978.

it should be also considered whether there is the possibility of the suppression of the junction temperature variation in a pulse duration or not, from the standpoint of the thermal design techniques. In addition, the maximum limitation of output power of diodes, and the reliability of diodes depend on the junction temperature of diodes. However, it has not yet been reported about what position the heat sink should be set for the pulse width, to sink heat generated in diodes efficiently in pulse operation. Thus, it is necessary to call for the knowledge of the transient response of the junction temperature in pluse-operated diodes.

Perlman has reported calculated transient responses of the temperature for an active rod, neglecting thermal influence of a heat sink, in addition to, neglecting temperature dependences of thermal constants in the rod [11]. Gibbons has reported calculated transient respenses of the temperature on the semi-infinite heat sink by considering only the spreading heat resistance, neglecting the thermal effect in the diode chip [12]. A typical device for pulse-operated diodes is composed of a united body of the diode chip with metallic contacts and semi-infinite heat sink. Thus, the above models can not be applied to the estimation of the thermal effects of the diode chip and heat sink for such device structure, since the thermal effects of the spreading thermal resistance in the heat sink is not taken into account in the Perlman model and of the thermal resistance in the diode chip in the Gibbons model. Olson has reported calculated transient responses of temperature rise in diamond-heat-sink IMPATT diode by using analogies of electrical circuits [13]. In this case, it is not so easy to calculate equivalent values of the elements in the analogous electrical circuit of time. The new model proposed takes into account both thermal effects of the diode chip and heat sink, in addition to temperature dependent thermal constants. In this model, the temperature is expressed by an analytical function for a united body of the diode chip with the metallic contacts and heat sink. Thus, by this model, we can rather easily estimate the transient responses and spatial distributions of the temperature in the diode, in comparison with the case of Olson model. In chapter 2, a physical model for typical diodes to be analyzed and the formulae to calculate transient responses and spatial distributions of temperature are presented. In chapter 3, turn-on and turn-off temperature transient responses are compared with ones calculated by using methods so far reported and also with the experimantal one, to show the validity of this analysis. In chapter 4, the effects of temperature dependencies of thermal constants on the responses are discussed. In chapter 5, the thermal effects of the metal contacts, chip area and chip length will be shown and discussed. In chapter 6, the useful relation between the position for the heat sink to be set and the operation pulse width is shown as the condition to have efficient heat-sink effect in the thermal design of diodes. In chapter 7, the possibility of suppression of a temperature variation during a pulse is discussed from the standpoint of thermal diode-design techniques. In chapter 8, summary and conclusions are presented.

2. Physical model and analysis

The simplified physical model for typical diodes under analysis is shown in Fig. 1. This

model is considered applicable as the thermal model to the cases of mesa diodes mounted upside down or right upside up on the heat sink. As well known, in these cases, the semiconductor substrate is removed by lapping, ethcing or other techniques to improve the heat sink efficiency. The heat sink effects due to thermal conduction through the lead wire, due to thermal radiation and due to thermal convection are assumed to be negligible in this model. This model is composed of three parts: a cylindrial semiconductor rod for a diode chip, a circular metallic contact having same area S as this rod, and a semi-infinite substrate for an ideal heat sink. The structure is assumed to be circularly symmetric about the x axis. The junction as the heat source is assumed to be located on the top surface of the rod. This source yields repetition pulse power P_{L1} with the magnitude P_1. The junction temperature and the temperature rise are denoted as T_1 and ΔT_1, respectively. The K and α with a number subscript are the thermal conductivity and diffusivity in each medium denoted as the subscript, respectively. The heat generated on the top surface of the rod flows through the semiconductor rod and metallic contact and reaches the heat sink. Thermal constants are assumed to be independent of temperature at the beginning of this analysis, but the temperature dependency will be taken into account in the next step, in which computer calculation is employed. For the model shown in Fig. 1, the following equation of linear flow of heat can be used,

$$\frac{\partial^2 T}{\partial x^2}=\frac{1}{\alpha}\frac{\partial T}{\partial t}=\frac{1}{KS}\frac{KS}{\alpha}\frac{\partial T}{\partial t} \tag{1}$$

where t is time and T is temperature. The equation is the same form as the equation (2) describing the voltage V in a distributed RC network as shown in Fig. 2.

$$\frac{\partial^2 V}{\partial x^2}=RC\frac{\partial V}{\partial t} \tag{2}$$

where R and C are the resistance and capacitance per unit length, respectively. The above thermal constants (K and α), T_1 and P_{L1} can be translated into the electrical constants due

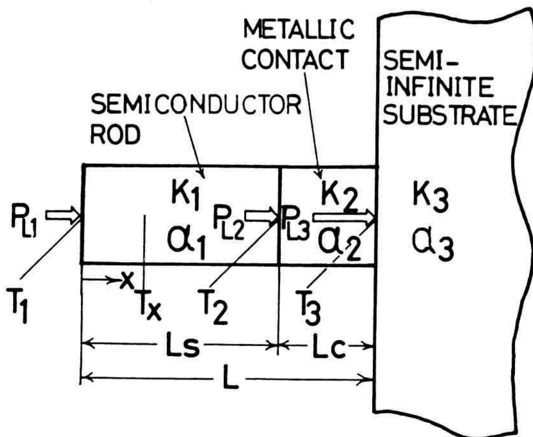

Fig. 1. Physical model for typical diodes.

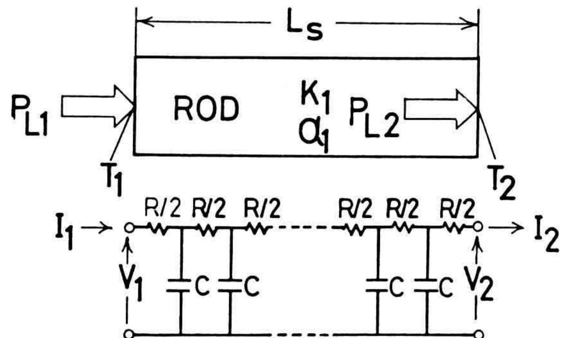

Fig. 2. Electrical analog of semiconductor rods.

to the analogy, as follows ; $1/KS=R$, $KS/\alpha=C$, $T_1=V_1$ and $P_{L1}=I_1$. The relation between the input (T_1, P_{L1}) and output signal (T_2, P_{L2}) in the rod with the length of L_s as shown in Fig. 2 is expressed as following :

$$\begin{bmatrix} T_1 \\ P_{L1} \end{bmatrix} = \begin{bmatrix} A_1 & B_1 \\ C_1 & D_1 \end{bmatrix} \begin{bmatrix} T_2 \\ P_{L2} \end{bmatrix} \tag{3}$$

$$A_1=\cosh(a_1L_s), \qquad B_1=\{\sinh(a_1L_s)\}/(a_1K_1S)$$
$$C_1=a_1K_1S\sinh(a_1L_s), \qquad D_1=\cosh(a_1L_s)$$
$$a_1=(j\omega_n/a_1)^{\frac{1}{2}}$$

where ω_n is the anbular frequency of the nth harmonic wave. The matrix expression for the structure of the semiconductor rod with the matallic contact with the length of L_c as shown in Fig. 1, is readily obtained as in (4) by the cascabde connection of the F matrix as in (3).

$$\begin{bmatrix} T_1 \\ P_{L1} \end{bmatrix} = \begin{bmatrix} A_1 & B_1 \\ C_1 & D_1 \end{bmatrix} \begin{bmatrix} A_2 & B_2 \\ C_2 & D_2 \end{bmatrix} \begin{bmatrix} T_3 \\ P_{L3} \end{bmatrix} = \begin{bmatrix} A & B \\ C & D \end{bmatrix} \begin{bmatrix} T_3 \\ P_{L3} \end{bmatrix} \tag{4}$$

$$A_2=\cosh(a_2L_c), \qquad B_2=\{\sinh(a_2L_c)\}/(a_2K_2S)$$
$$C_2=a_2K_2S\sinh(a_2L_c), \qquad D_2=\cosh(a_2L_c)$$
$$a_2=(j\omega_n/a_2)^{\frac{1}{2}}.$$

Thus, T_1 becomes

$$T_1=\frac{A\dfrac{T_3}{P_{L3}}+B}{C\dfrac{T_3}{P_{L3}}+D}P_{L1}. \tag{5}$$

The rod described above is connected to the semi-infinite substrate as shown in Fig. 1, the explicit expression for the T_3/P_{L3} in (5) is obtained as follows. For the case when a step-function power P_{L3} having the magnitude of P_3 is applied to the surface of the semi-infinite substrate as shown in Fig. 3, Gibbons [12] has extracted the analytical expression as a function of time for the transient temperature T_3 at the center of the circular disk by using Carslow's theory, as follows,

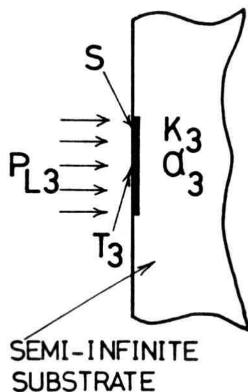

Fig. 3. Physical model for heat sinks.

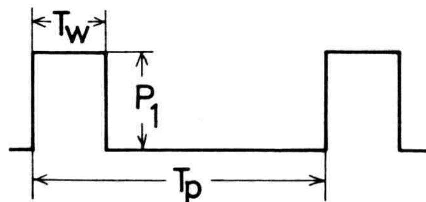

Fig. 4. Waveform of power-pulse supplied.

$$T_3=\frac{P_3(\alpha_3)^{\frac{1}{2}}}{K_3S}\left[2\left(\frac{t}{\pi}\right)^{\frac{1}{2}}-2\left(\frac{t}{\pi}\right)\exp\left(-\frac{S}{4t\pi\alpha_3}\right)\right.$$
$$\left.-\left(\frac{S}{\pi\alpha_3}\right)\operatorname{erfc}\left\{\frac{1}{2}\left(\frac{S}{\pi\alpha_3 t}\right)\right\}\right]. \tag{6}$$

The transfer function T_3/P_{L3} is given as in (7) as a function of an angular frequency, by the Laplace transform of (6) [15],

$$\frac{T_3(j\omega_n)}{P_{L3}(j\omega_n)}=\frac{1}{K_3S}\left(\frac{\alpha_3}{j\omega_n}\right)^{\frac{1}{2}}\left[1-\exp\left\{-\left(\frac{j\omega_nS}{\pi\alpha_3}\right)^{\frac{1}{2}}\right\}\right]. \tag{7}$$

Thus, the analytical expession as a function of frequency for the transient temperature response at the junction is newly obtained by substituting (7) into (5). The power supplied can be assumed as rectangular pulse shown in Fig. 4, since the power dissipation in the junction keeps constant during a pulse for diodes usually used. Such assumtion has been also made by Gibbons [12] and Olson [13]. The pulse power can be expressed by Fourier expansion form as in (8)

$$P_{L1}=\frac{P_1}{m}+\sum_{n=1}^{\infty}\left\{\frac{2P_1}{n\pi}\sin\left(\frac{n\pi}{m}\right)\cos\omega_n t\right\} \tag{8}$$
$$m=\frac{T_P}{T_W}.$$

Thus, the equation to express the transient of the junction temperature T_1 is given as follows;

$$T_1=\frac{P_1L_s}{mSK_1}+\frac{P_1L_c}{mSK_2}+\frac{P_1}{mK_3}\left(\frac{1}{\pi S}\right)^{\frac{1}{2}}$$
$$+\sum_{n=1}^{\infty}\left\{\left|\frac{A\left(\frac{T_3}{P_{L3}}\right)+B}{C\left(\frac{T_3}{P_{L3}}\right)+D}\right|\frac{2P_1}{n\pi}\sin\left(\frac{n\pi}{m}\right)\cos\left(\omega_n t+\phi_n\right)\right\} \tag{9}$$

where

$$\phi_n=\tan^{-1}\left[Im\left\{\frac{A\left(\frac{T_3}{P_{L3}}\right)+B}{C\left(\frac{T_3}{P_{L3}}\right)+D}\right\}\Big/Re\left\{\frac{A\left(\frac{T_3}{P_{L3}}\right)+B}{C\left(\frac{T_3}{P_{L3}}\right)+D}\right\}\right].$$

The last term in the above (9) represents the temperature rise due to the AC component in all of the heat paths. The other terms are due to DC components; the first term is due to the semiconductor rod, the second term due to the metallic contact, and the third term due to the spread impedance in the substrate. Here, P_1 in the first and second term in (9) is devided by the cross area S of the rod, and P_1 in the third term is devided by $S^{1/2}$. If duty cycle of the pulse applied is as small as a case when a single pulse is applied, the third term can be neglected since the term becomes sufficiently smaller than the AC component. Thus, in such case, the applied power can be normalized by the area S.

Furthermore, the expressions to describe the spatial temperature T_x and power P_{Lx} at the position separated by x from the thermal source in the rod given by modifying the inverse matrix of (3) as follows;

$$T_x = (D_x T_1 - B_x P_{L1}) / (A_x D_x - B_x C_x)$$
$$P_{Lx} = -C_x T_1 + A_x P_{L1} \qquad (10)$$

where, A_x, B_x, C_x and D_x are given by replacing L_s in (3) by x. T_1 for P_{L1} can be known previously by computing (9), so T_x and P_{Lx} can be obtained by computing (10).

In the above theory, thermal constants have been assumed to be independent of temperature. But, thermal constants of Si and GaAs depend on the temperature as described in Appendix. In this paper, the temperature dependence is introduced by a numerical analysis technique in the computing process, as the following describing. The temperature is different at each position in the rod, so the values of thermal constants are also different at each position. So, the rod is decomposed into many thin laminae in x direction, in which the lamina width is varied complying with the magnitude of the spatial temperature gradient, and the thermal constants are assumed to be uniform within the each thin lamina. The values of thermal constants in each lamina are decided from the spatial temperature already calculated by using (10) about each lamina at time before one mesh of time on the computing.

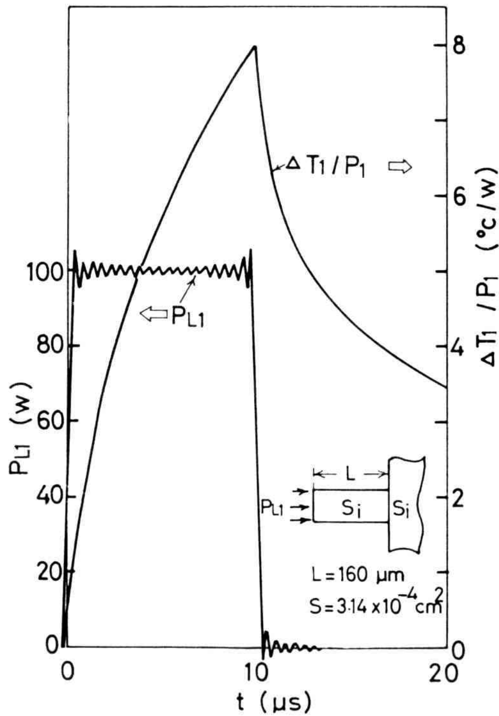

Fig. 5. An example of pulse waveform and transient temperature response computed from this model.

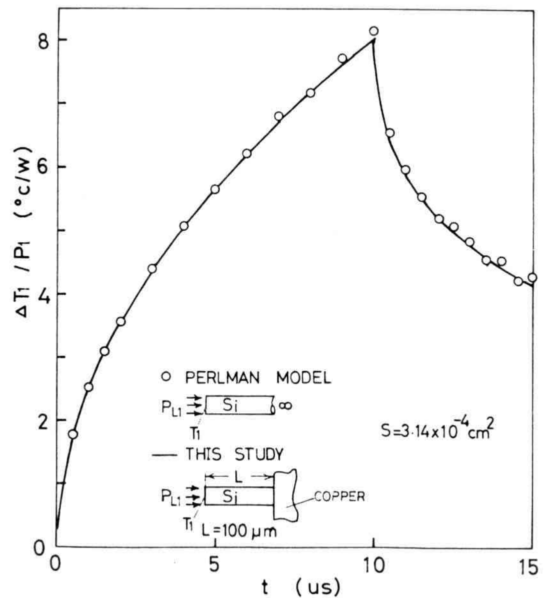

Fig. 6. Comparison between turn-on and turn-off temperature responses calculated from this model and that from the Perlman model.

3. Validity of analysis

In order to compose a rectangular pulse waveform from the Fourier expansion of (8), the higher harmonics must be used. On the other hand, the higher harmonics should be limited since short computing time is desired. As an example, Fig. 5 shows the rectangular pulse form with the pulse width of 10 μs and repetetion frequency f_p of 1 kHz, and the transient temperature response computed by taking the harmonics of 2000 orders. The influence of limitation of the higher harmonics softens slightly the rise and fall waveform as the pulse sown in Fig. 5 and yields a vibrating form with the small amplitude in the flat top of the pulse as seen in Fig. 5. The influence of the former is small on the aspect of temperature as seen in the temperature transient in Fig. 5. The influence of the latter scarcely appears in the temperature transient as seen in Fig. 5. The supplied pulse is expressed by the periodic pulse as in (8). If one desire to obtain a single pulse, it is obtained by decreasing the duty cycle. If the duty cycle is smaller than 1%, e.g., a pulse with the repetetion frequency of 1 kHz and pulse width of 10 μs, can be regarded as a single pulse completely. This is confirmed from the computing result that the temperature at the end time of the cooling cycle equals to the ambient temperature, as seen in Fig. 5.

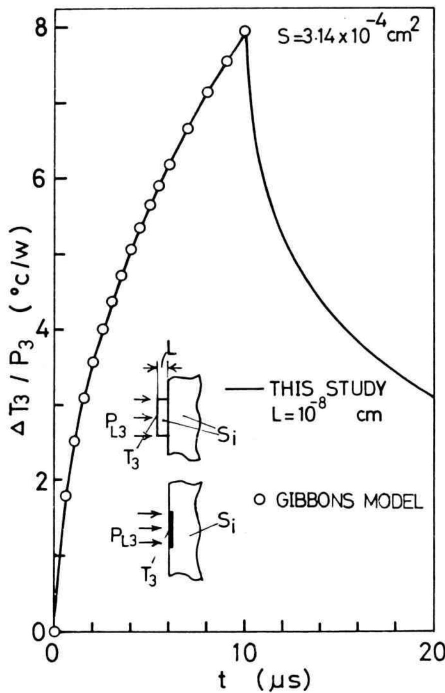

Fig. 7. Comparison between turn-on temperature transient calculated from this model and that from the Gibbons model.

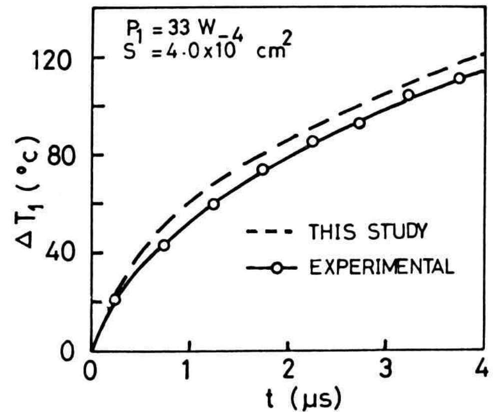

Fig. 8. Comparison between experimental and calculated turn-on temperature transients. The calculation was made from this model with temperature dependent thermal constants.

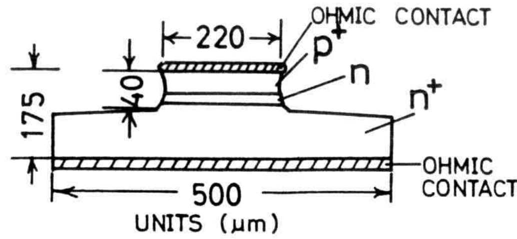

Fig. 9. Diode structure used for the measurement.

To show the validity of this analysis, Fig. 6 shows the comparison between the turn-on and turn-off transient temperature calculated by Perlman's analysis and calculated by the analysis based on (8) under the condition that the calculated result fits his model†. Fig. 7 shows the comparison between the result calculated by Gibbons' analysis and that by this analysis. The results by this analysis are in good agreement with that obtained from Perlman's and Gibbons' analysis. Thus, this analysis turns out to be valid. Furthermore, Fig. 8 shows the comparison between the turn-on transient response of the temperature calculated from this theory and the experimantal data. The diode used for the measurement

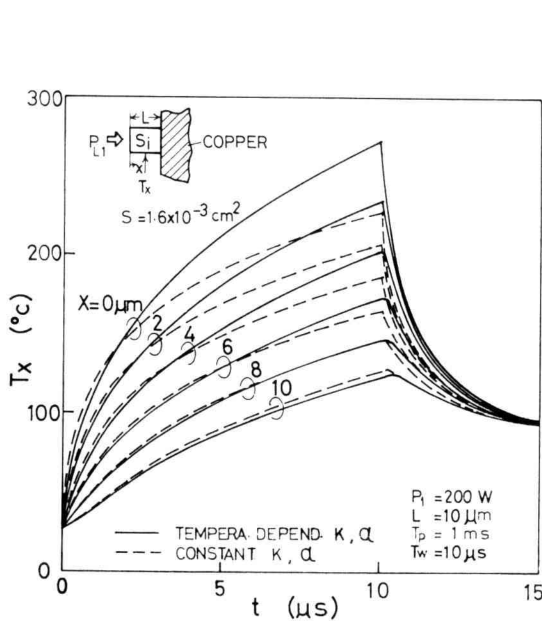

Fig. 10. Comparison between turn-on and turn-off temperature transient calculated from this model with and without temperature dependent thermal constants.

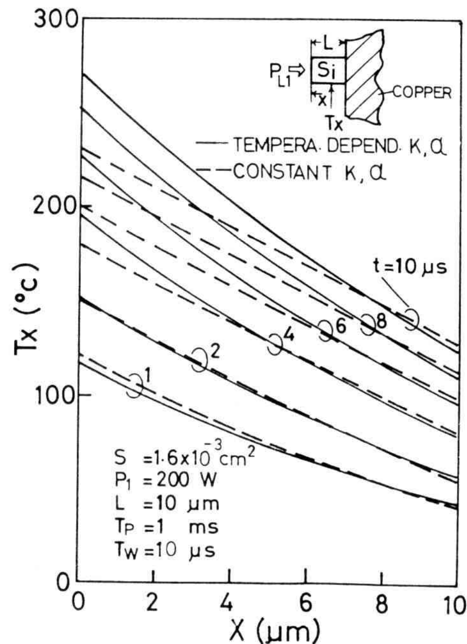

Fig. 11. Comparison between spatial temperature distribution calculated from this model with and without temperature dependent thermal constants.

† His model did not take into account the thermal effect of the heat sink, so the rod length was taken to be long to neglect the effect in this model.

is the Si mesa type diode with a Si substrate of a definite size as shown in Fig. 9. This diode has been used for TRAPATT oscillation [1], [4], [5], [9]. The experimental data were obtained from the measurement of the breakdown voltage due to only the temperature change, removing the influence due to the space change effect, in the supply of the single pulse power with a pulse width of 4 μs [9]. We can see that the theoretical result is in agreement with the experimental one, in a certain extent as is seen in Fig. 8. Thus, it can be said that this analysis is reasonable.

4. The effect of temperature dependencies of thermal constants

To know the temperature effect due to the temperature dependencies of thermal constants, the comparison is shown in Figs. 10 and 11, between the response calculated by using the constant thermal constants at 80℃ and ones calulated by using the temperature dependent thermal constants. Fig. 10 shows the transient response of the temperature at various positions in the rod. Fig. 11 shows the spatial temperature distribution within the rod for the elapsed time. In the high temperature region, there is a difference between both temperature with and without variable thermal constants, as is known from the figures. The maximum safe operating temperature of diodes is abous 300℃ for Si and 450℃ for GaAs of the impurity concentration of 10^{15} cm^{-3} in the active region of the diodes. But, the maximum temperature in the diode for practical use is usually limited at about 200℃ from the view point the reliability. In such a case, the relative difference between both temperatures is about 7% at the maximum point as seen in the figures. So, it can be said that if the range of the

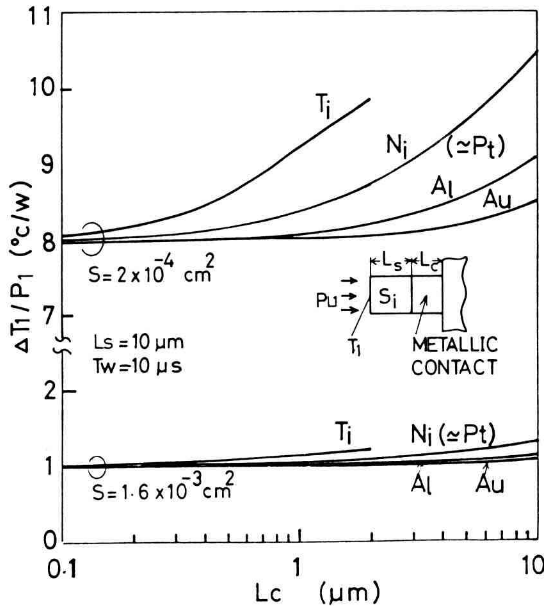

Fig. 12. Contact-thickness dependence of thermal resistance for various metallic contacts.

Table 1 Thermal conductivity and diffusivity in heat sink materials used for calculation.

Material		K (W/°ccm)	α (cm^2/s)
Copper		4.0	1.14
Diamond IIa		22.0	1.01
Beryllia		2.1	0.60
Titanium	(Ti)	0.2	0.0086
Platinum	(Pl)	0.69	0.24
Nickel	(Ni)	0.84	0.21
Gold	(Au)	2.97	1.18
Aluminum	(Al)	2.04	2.81

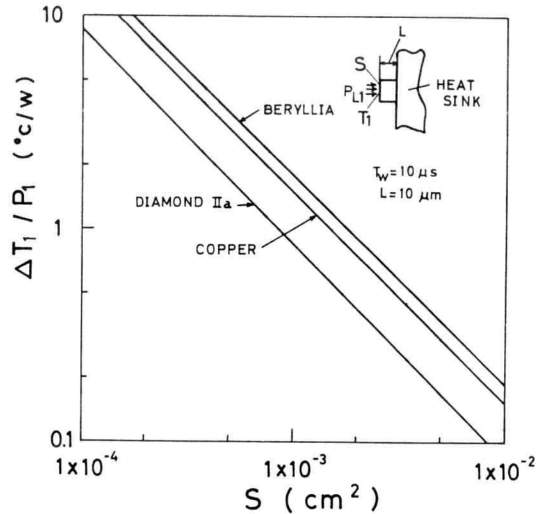

Fig. 13. Diode chip area dependence of thermal resistance for various heat sink materials.

temperature rise is limited in about 200℃, the results obtained by neglecting the temperature dependencies, do not cause a large error. The temperature dependencies in GaAs are slightly smaller than ones in Si (refer to Fig. 22), so the neglection of them do not also cause a large error. In the case of utilizing the constant thermal constants, we can also define a transient thermal resistance $\varDelta T_1/P_1$ which is function of time as defined already by Gibbons [11]. All of the figures in this paper, in which the ordinates is represented by $\varDelta T_1/P_1$ show the results calculated by using the constant thermal constants at 80℃.

5. Temperature effect of metallic contact, chip area and chip length

A metallic contact is used as a ohmic contact of a diode and as a mounting of diode chip on a heat sink. We consider a model in which such metals as Au, Pt. Al and Ti is put between the diode chip and the heat sink, as shown in Fig. 1. The contact-thickness dependence of the thermal resistance for various metallic materials is shown in Fig. 12 for the pulse width of 10 μs and the Si rod length of 10 μm. The values of the thermal constants of the metals are given in Table 1. The increase of the thermal resistance due to those contacts is small except for due to Ti as seen in Fig. 12.

Fig. 13 shows the rod area dependence of the thermal resistance for various heat sink materials in a case of pulse width of 10 μs. The values of the thermal constants of the heat sink are given in Table 1. The thermal resistance decreases in proportion to the rod area. This indicates that the thermal resistances in the figures through this paper can be normalized by dividing by the area S.

Fig. 14 and 15 show the chip length dependence of the thermal resistance for various pulse widths in Si chip with copper and diamond IIa heat sinks, respectively. The chip length

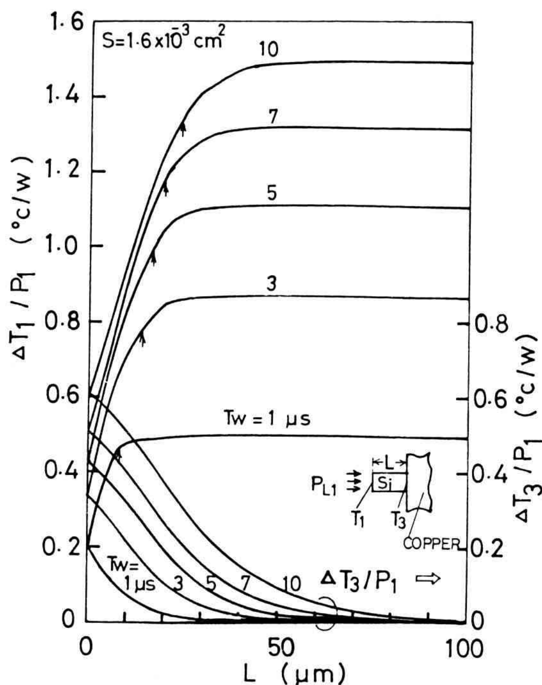

Fig. 14. Source-sink length dependence of thermal resistance for various pulse width in diode chip with copper heat sink.

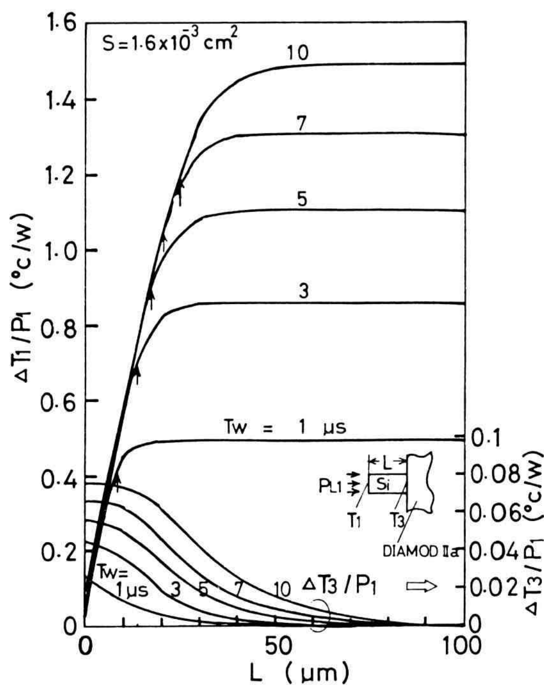

Fig. 15. Source-sink length dependence of thermal resistance for various pulse width in diode chip with diamond IIa heat sink.

dependence of the temperature rise ΔT_3 on the heat sink is also shown in the same figures. The thermal resistance increases with increase of the chip length, and it saturates in a certain chip length. It is noted that the chip lengths where the saturation occur depends on pulse width but the saturated values of the thermal resistance are almost the same for both copper and diamond IIa heat sinks. That is, they do not virtually depend on the thermal character of the heat sink material but on that of the chip itself.

6. Setting position condition of heat sink

The effect of a heat sink in a pulse operation is different from that in a CW operation. For example, if a heat sink is located in the far position separated from the thermal source and if a pulse width is not so long, the thermal flux does not yet arrive to the heat sink during the heating hycle, so the sink effect of the heat sink disappers, as is predicted from Fig. 14 and 15. This phenomenon is verified more apparently by Fig. 16 and 17. Fig. 16 shows an example of the temperature transient at the various positions inside the rod and Fig. 17 shows the spatial temperature distribution for the time elapsed after the pulse width of 10 μs is applied. These figures indicate that the temperature at the far posotion separated from the thermal source does not rise during the heating cycle. Thus, to expect the sink effect of the heat sink, the position to set the heat sink should be determined by the width of the pulse

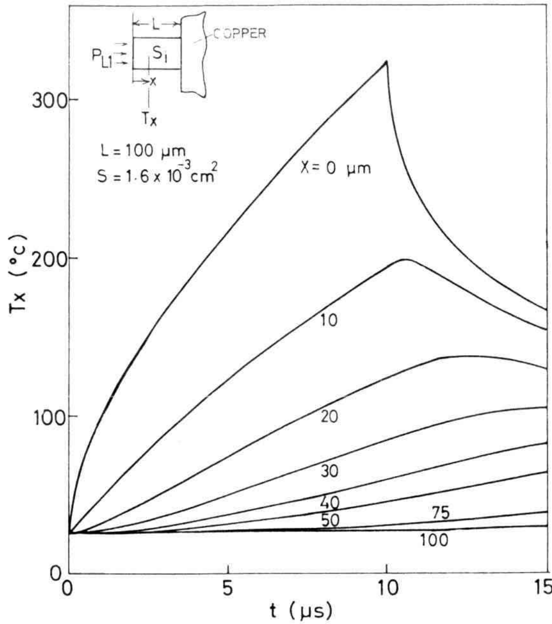

Fig. 16. Temperature transient at various position in a semiconductor rod.

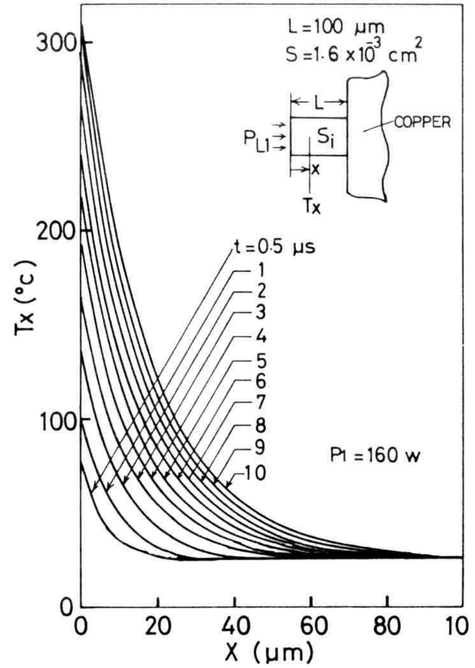

Fig. 17. Spatial temperature distributions in a semiconductor rod for a elapsed time.

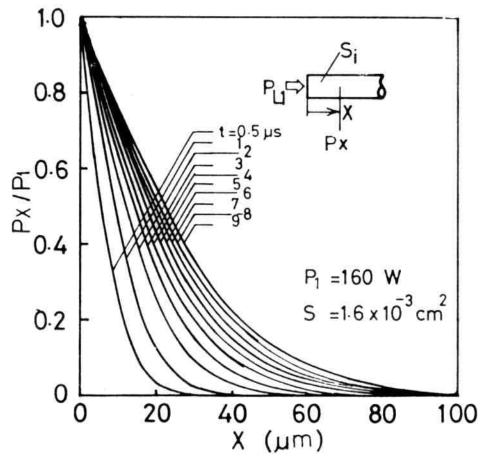

Fig. 18. Spatial power distribution in a semiconductor rod for a elapsed time (P_x is normalized by the power P_1).

given. Fig. 14 and 15 have shown that the thermal resistance becomes constant in a certain chip length, and then, the heat sink effect disappears, and the length is different due to the pulse width. This phenomenon is basically caused by the definite propagation speed of the thermal or power flux through the semiconductor chip. Fig. 18 shows an example of the normalized power distribution in the chip for elapsed time after pulse-on. In order to expect

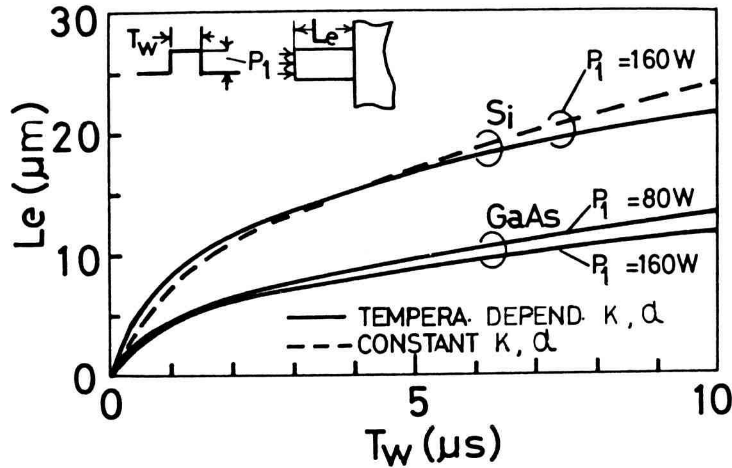

Fig. 19. Relation curves between source-sink length and pulse width, to get efficiently sink effect due to the heat sink.

the sink effect due to the heat sink, the sufficient power flux must reach the surface of the heat sink. So, it was assumed that, when the half of supplied power flux reaches the surface of the heat sink, the sink effect begins to appear strongly. The length Le between the thermal source and the heat sink, to satisfy this assumption for the operation pulse width of $T_{w'}$ is obtained from Fig. 18. The relation between the length and the pulse width for Si and GaAs chips is shown in Fig. 19. The arrow signs in Fig. 14 and 15 show the thermal resistance decreased due to the sink effect of the heat sink located at the position determined by this relation. This relation corresponds to the effect to decrease the thermal resistance by about 10% for a copper and 20% for a diamond IIa heat sink, due to setting of the heat sink, as known from Fig. 14 and 15, respectively. The broken line in Fig. 19 shows the result using the constant thermal constants. The line in GaAs is under the line in Si since the thermal diffusivity of GaAs is smaller than that of Si. The difference between the line at $P_1=80$ W and the one at 160 W is smaller as seen in the figures. This difference depends on the temperature dependency of the thermal diffusivity. Because the diffusion speed of the power in the rod is dependent on the thermal diffusivity which corresponds to the inverse of the time constant CR in electrical CR circuits. These curves are approximated by the fitting function $Le=(\alpha_e T_w)^{\frac{1}{2}}$ in which α_e is the thermal diffusivity at 150℃. Thus, the result in Fig. 19 is virtually independent of the chip area and the magnitude of the pulse power. Thus, it can be said that the heat sink must be set at the position inside the region under the line in Fig. 19 for the pulse width given. For instance, if one desires the heat-sinked Si diode operation with the pulse width of 5 μs, one should set the heat sink at the position inside 5 μm from the heat source.

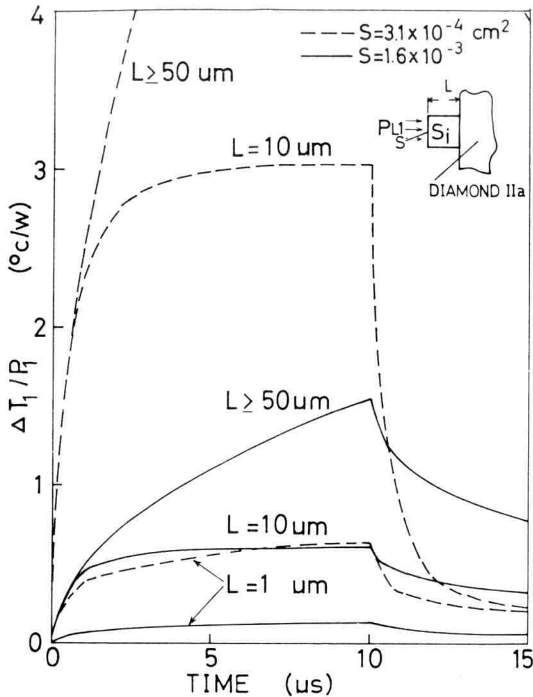

Fig. 20. Temperature transient response for various source-sink length in diode chip with diamond IIa heat sink.

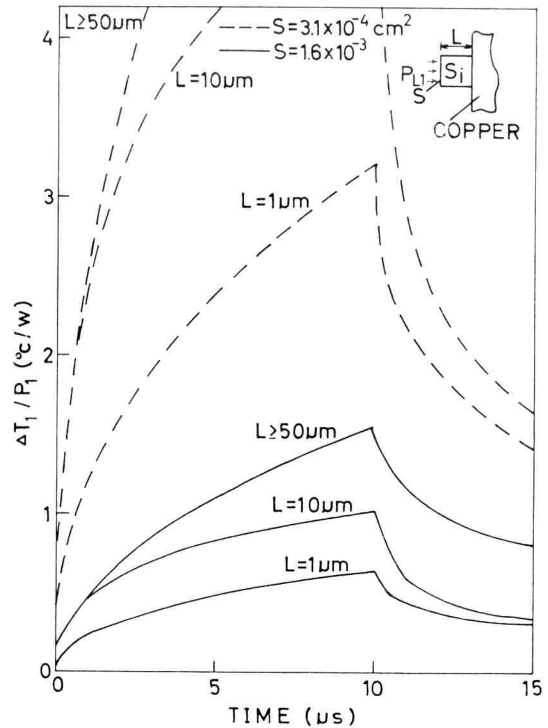

Fig. 21. Temperature transient response for various source-sink length in diode chip with copper heat sink.

7. Suppression of temperature variation during a pulse

Fig. 20 and 21 show the the transient response of the junction temperature for various chip lengths in the diode chip with the diamond IIa and copper heat sink, respectively. When the heat sink is at the place ($L=1$ μm) close to the thermal source, the temperature variation during a pulse is small, since the temperature rise is mainly characterized by the heat sink itself. Because the thermal flux arrives at the heat sink in short time. On the other hand, in the case of $L=50$ μm, the temperature variation is large, since the temperature rise is mainly characterized by the semiconductor chip itself. Because the thermal flux does not yet arrive at it within the pulse width, as discussed in chapter 5 and 6. The curve of $L=10$ μm shows that the temperature rises rapidly in short time elapsed after turn-on, and after then the gradient of the curve approaches the one in $L=1$ μm, so that the temperature variation is small during remaining pulse width except for the instant rise. This phenomenon is characterized by the combining the propagation delay time of heat throughout the semiconductor chip with the sink effect of the heat sink. Therefore, there is a turning time when the gradient of the curve changes irregularly. The turning time corresponds approximately to the pulse width determined from the curve in Fig. 19. This means that the turning time

corresponds to the time when the sink effect begins to occur effectively. Thus, the variation becomes small during the remaining pulse width, though the temperature varies until the turning time. This effect is more remarkable in the diamond IIa than in the copper heat sink as seen in Fig. 20 and 21. In a case of GaAs, the turning time is estimated to be 6.5 μs for the chip length of 10 μm, as seen in Fig. 19. If one expects such effect for the pulse width of 10 μs in GaAs, the chip length must be less than 5 μm as is known from Fig. 19. The effect will be also expected from Fig. 19 for such longer pulse width as several tens of micro-seconds even if the chip length is 10 μm.

8. Summary and conclusions

Here, we summarize the above discussions and conclude, as follows.

(1) A thermal model for a diode chip with a heat sink has been proposed to estimate transient responses and spatial distributions of temperature in pulsed microwave oscilllation diodes.

(2) We compared beteen, turn-on and turn-off temperature transients calculated by this model, and that by published methods and that obtaied experimentally.

(3) It has been shown on the basis of the comparison between the results with and without the temperature dependent thermal constants, that temperature transients calculated by using the constsnt thermal constants does not contain a large error over the ranging from 0 to 200℃.

This in a useful conclusion since it indicates to make the analysis simple and the computing time short.

(4) The metal-contact-thickness dependence, the chip area dependence, and chip length dependence, of the thermal resistance have been shown.

(5) The relation between the source-sink length and the pulse width has been shown for Si and GaAs diode chip ; the relation allows us to find the setting position of the heat sink, as the condition to sink heat efficiently, for the pulse width applied. This is useful for the thermal design of pulsed diodes.

(6) The possibility of the suppression of the variation of the junction temperature during a pulse by thermal diode design techniques has been proposed. It has been shown that the possibility can be expected when the diamond IIa heat sink is put at the position in which the turning time occurs at the early elapsed time in the pulse width supplied. The turning time can be determined from the relation given in Fig. 19.

(7) In a case when the junction is embeded within the semiconductor rod not the end surface, the transient response of the junction temperature can be obtained by connecting parallel the each thermal resistance calulcated from this model for the each medium seen from the junction. In this case, the spatial temperature distribution can be also calculated by this calculation method.

Acknowledgement

The author wishes gratefully to thank Prof. S. Furukawa of Tokyo Institute of Technology for his useful advices. He is also grateful to Prof. G. Kishi of same Institute for his help in using the computer.

References

1) S. Furukawa, Y. Ogita and K. Honjo, Paper of Technical Group on Microwaves, Inst. Electro. Communi. Eng. Japan, MW74-45 (1974)
2) B.J. Udelson and R.E. Hines, Proc. IEEE (letters) **57**, 2091 (1969)
3) M. Kotani, S. Mitsui and K. Shirahata, Paper of Technical Group on Electron Devices, Inst. Electro. Communi. Eng. Japan, **77**, No. 39 (1997)
4) Y. Ogita, S. Furukawa and K. Honjo, Trans. Inst. Electro. Communi. Eng. Japan, **59-B**, 333 (1976), avalable in English in Electronics and Communications in Japan, same data, **59**, 6, 86 (1976)
5) K. Honjo, Y. Ogita and S. Furukawa, Trans. Inst. Electro. Communi. Eng. Japan, **59-B**, 431 (1976), avaialble in English in Electoronics and Communication in Japan, same data, **59**, 854 (1976)
6) Y. Ogita and K. Honjo, Research Reports of Ikutoku Technical Univ. **B-4**, 23 (1980)
7) K. Ogiso, I. Shima and D. Taketomi, Paper of Technical Group on Electron Devices, Inst. Electro. Communi. Eng. Japan, **77**, No. 212 (1978)
8) E.D. Bullimore, B.J. Dowing and F.A. Myers, Electronics Lett., **10**, 220 (1974)
9) Y. Ogita and S. Furukawa, Trans. Inst. Electro. Communi. Eng. Japan, **E61**, 73 (1978)
10) T. Suzuki and K. Sekido, Nat'l Conv. Rec. of Inst. Electro. Communi. Eng. Jpapan, No. 333, (March 1975)
11) B.S. Perlman, RCA Review, **30**, 637 (1969)
12) G. Gibbons, Solid-St. Electron., **13**, 799 (1970)
13) H.M. Olson, IEEE Trans. Electron Dev., **ED-23**, 494 (1976)
14) H.S. Carslaw and J.C. Jaeger, Conduction of heat in solids, p. 255, Oxford Univ. Press, London (1959)
15) R.V. Churchill, Operational mathematics, p. 464, MaGraw-Hill Kogakusha, Tokyo (1972)
16) H.R. Shanks, P.D. Maycock, P.H. Sidels and G.C. Danielson, Physical Rev., **130**, 1743 (1963)
17) P.D. Maycock, Solid-St. Electron., **10**, 161 (1967)

Appendix

The following expressions have been used in this analysis for the thermal conductivity and the thermal diffusivity as a function of temperature in unit (℃) obtained by curve-fitting experimental data over the ranging from 0 to 350℃ published in refernces [16], [17], as shown in Fig. 22.

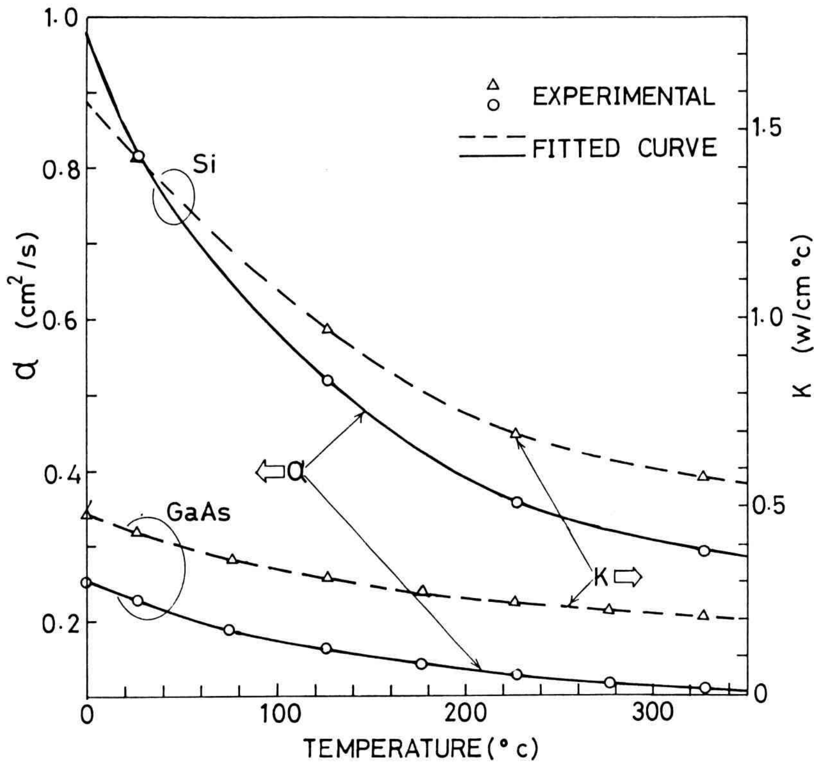

Fig. 22. Temperature dependences of thermal constants for Si and GaAs.

For Silicon:

$$K=8.67\times10^{-6}T^2-5.86\times10^{-3}T+1.58$$

$$\alpha=-1.70\times10^{-8}T^3+1.56\times10^{-5}T^2-5.40\times10^{-3}T+0.983$$

For Gallium Arsenide:

$$K=-4.17\times10^{-9}T^3+4.50\times10^{-6}T^2-1.86\times10^{-3}T+0.485$$

$$\alpha=0.522K$$

These functions are expressed by the solid and the broken lines in Fig. 22.